Supporting Information

Green Synthesis of δ-Lactam from Biomass-Derived 4-Hydroxy-6-Methylpyridin-2(1H)-one

1. Experimental

Materials and chemicals

Ruthenium (III) chloride (Ru: 37-40%), nickel (II) nitrate hexahydrate (98%), copper (II) nitrate trihydrate (99.9%) and hydrogen hexachloroplatinate (IV) hydrate (Pt: 40%) were provided by Inno-chem Ltd (Beijing, China). Palladium chloride (Pd: 59-60%), iron (III) nitrate nonahydrate (99.9%) and cobalt nitrate hexahydrate (99.9%) were purchased from the Meryer CO. LTD (Shanghai, China). 4-Hydroxy-6-methyl-2-pyrone (TAL, 98%), 6-methylpiperidin-2-one (MPO, ≥95%) and diisopropylamine (DPA) were obtained from Aladdin (China). MeOH, EtOH, 1-PrOH, 2-PrOH, 2-BuOH, *t*-BuOH, cyclohexanol, *t*-amyl alcohol and ammonia solution (25-28%) were provided by J&K Scientific Ltd (China). All the chemical reagents were used as received without further purification. Ketjenblack, EC-300J (carbon support) was purchased from Yilongsheng Energy Technology Co. Ltd (Suzhou, China). Mesoporous carbon (CMK-3, specific surface area≥800 m^2/g, pore size: 5-7 nm) was purchased from Xianfeng XF Nano Materials Technology Co. Ltd (China). The other catalyst supports like γ-Al_2O_3 and H-Y zeolite (Si: Al= 5:3) were provided by Energy Chemical (China). Pd (10 wt.%)/C and Pt (10 wt.%)/C were provided by Aladdin (China).

Catalyst Preparation:

The carbon supported Ni-Ru bimetallic catalysts were prepared *via* co-impregnation using metal precursors $RuCl_3$ and $Ni(NO_3)_2{\cdot}6H_2O$. Specifically, a calculated amount of metal precursor was first dissolved into a given amount of H_2O (2 mL), then slowly added the carbon supported (200 mg) under stirring. The obtained solid were dried at 80 °C overnight under vacuum. The dried catalysts were activated under H_2/Ar (H_2:

10%) atmosphere at 500 ºC/3 h. The mono-metallic Ni/C and Ru/C were synthesized by the similar impregnation method.

The other bimetallic catalysts like Ni-Pd/C, Ni-Pt/C, Cu-Ru/C, Fe-Ru/C and Co-Ru/C were prepared from the corresponding metal precursor through the above-mentioned procedures.

Catalytic Reaction:

Transfer hydrogenation/hydrogenolysis of HMPO to MPO with 2-PrOH

4-Hydroxy-6-methylpyridin-2(1H)-one (HMPO) was prepared through the amino-lysis of biomass-derived triacetic acid lactone (TAL) according to the reported method [1]. The catalytic reactions were carried out in a 15 mL Teflon-lined stainless-steel autoclave. In a typical experiment, catalyst (60 mg), HMPO (0.1275g, 1 mmol) and 2-PrOH (2 mL) were added into the autoclave. The autoclave was sealed and purged with N_2 three times to remove residual air. The catalytic reaction was performed at desired temperature and nitrogen pressure under magnetic stirring of 835 rpm. The reaction was stopped after certain periods of time, and the reactor was cool down in an ice bath instantly. The liquid phase was separated from the mixture by filtration. The qualitative analysis of reaction products was carried out on a GC-MS system (Agilent 7890A-5975C), and the quantitative analysis was conducted on a GC system (Agilent 8890B) equipped with an HP-5 column and an FID detector. Decane was used as an internal standard.

In the recycling experiments, the used catalyst was separated by centrifugation and washed with 2-PrOH several times, and was reduced at 500 ºC for 3 h under H_2/Ar (H_2:10%) atmosphere after drying overnight at 80 ºC under vacuum. The recovered catalyst was reused for the next cycle.

Catalyst Characterization:

Powder X-ray diffraction (XRD) patterns were obtained on a Rigaku Ultima IV X-ray diffractometer using Cu Kα radiation at 35 kV and 25 mA (λ = 1.5405 Å) over a 2θ ranging from 5° to 90 ° at a scanning speed of 5°/min.

Transmission electron microscopy (TEM) was performed on a JEOL JEM-2100

microscope at an accelerating voltage of 200 kV.

X-ray photoelectron spectroscopies (XPS) were carried out using Al kα (hv = 1486.36 eV) radiation with a Thermo Scientific K-Alpha spectrometer. The peak positions were referenced internally to the C 1s peak at 284.6 eV.

The metal contents of the catalysts were determined by inductively coupled plasma atomic emission spectrometry (ICP-AES).

Nitrogen adsorption-desorption analysis was carried out at 77 K using a BEL-SORP-MAX adsorption analyzer. The samples were degassed at 300 °C for 3 h under vacuum before the measurement. The specific surface areas were obtained by the Brunauer-Emmett-Teller (BET) method.

H_2-temperature programmed reduction (H_2-TPR) was carried out on a Chemisorption Analyzer (Micromeritics AutoChem II 2920) equipped with a thermal conductivity detector (TCD). For H_2-TPR analysis, about 60 mg of sample was used for each measurement and pretreated in an Ar flow at 200 °C for 2 h. TPR was initiated from 50 °C to 700 °C at 10 °C/min with a mixture flow of 10% H_2/Ar (20 mL/min).

2. Supplementary figures and tables

Table S1 ICP-AES analysis results of mono- and Ni-Ru bimetallic catalysts.

Ent.	Catalysts	Ru(wt.%)	Ni(wt.%)
1	Ru/C	2.71	-
2	Ni_1-Ru_{10}/C	4.07	1.18
3	Ni_2-Ru_{10}/C	3.92	1.77
4	Ni_3-Ru_{10}/C	3.65	2.32
5	Ni_4-Ru_{10}/C	4.14	3.16
6	Ni_5-Ru_{10}/C	4.64	3.74
7	Ni_3-Ru_{10}/CMK-3	3.56	3.37
8	Ni_3-Ru_{10}/H-Y	2.13	2.41

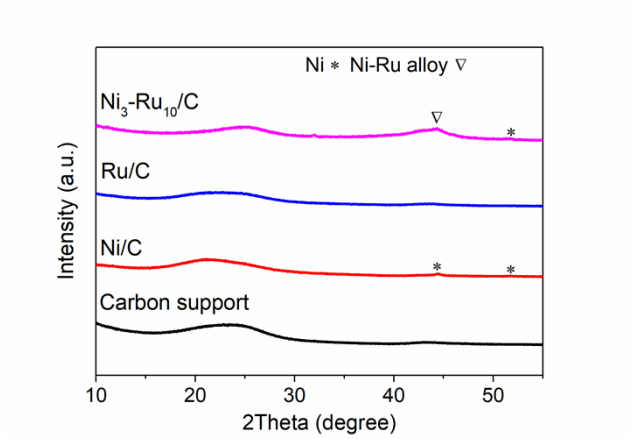

Fig. S1 XRD patterns of different supported catalysts on carbon support.

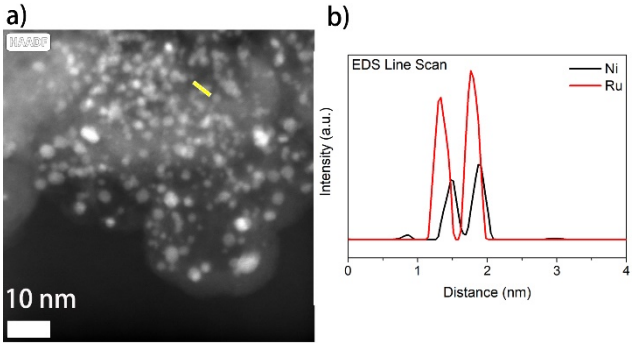

Fig. S2 The HADDF-STEM image (a) and the corresponding EDS line scan (b, marked by yellow line in the figure a) of Ni_3-Ru_{10}/C catalyst.

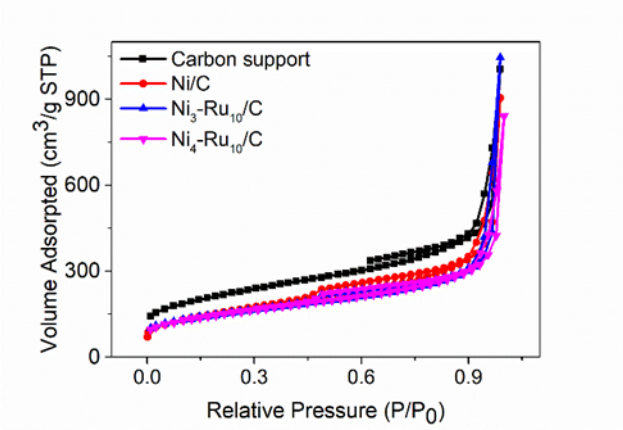

Fig. S3 N_2 adsorption-desorption isotherms of supported monometallic, bimetallic Ni-Ru catalysts and carbon support.

Table S2 Porosity properties of the mono- and bimetallic catalysts.

Ent.	Sample	Surface area (m^2/g)[a]	Total Pore volume (cm^3/g)[b]	Pore size (nm)[c]
1	Carbon Support	761.9	1.55	5.8
2	Ni/C	546.0	1.40	3.8
3	Ni_3-Ru_{10}/C	537.7	1.52	3.8
4	Ni_4-Ru_{10}/C	528.6	1.30	3.8

a) Surface area was calculated by the Brunauer–Emmett–Teller (BET) method; b) Total pore volume was obtained using the adsorption branch of the N_2 isotherm at $P/P^0 = 0.99$; c) Average pore diameter was determined from the local maximum of the BJH distribution of pore diameters obtained in the adsorption branch of the N_2 isotherm.

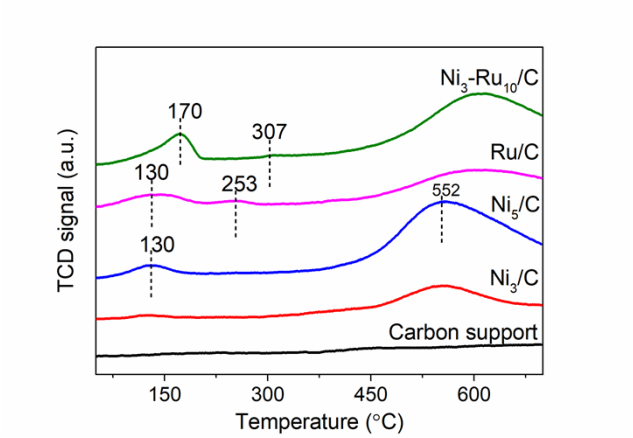

Fig. S4 H_2-TPR profiles of bimetallic Ni-Ru catalyst, monometallic Ru or Ni catalysts and carbon support.

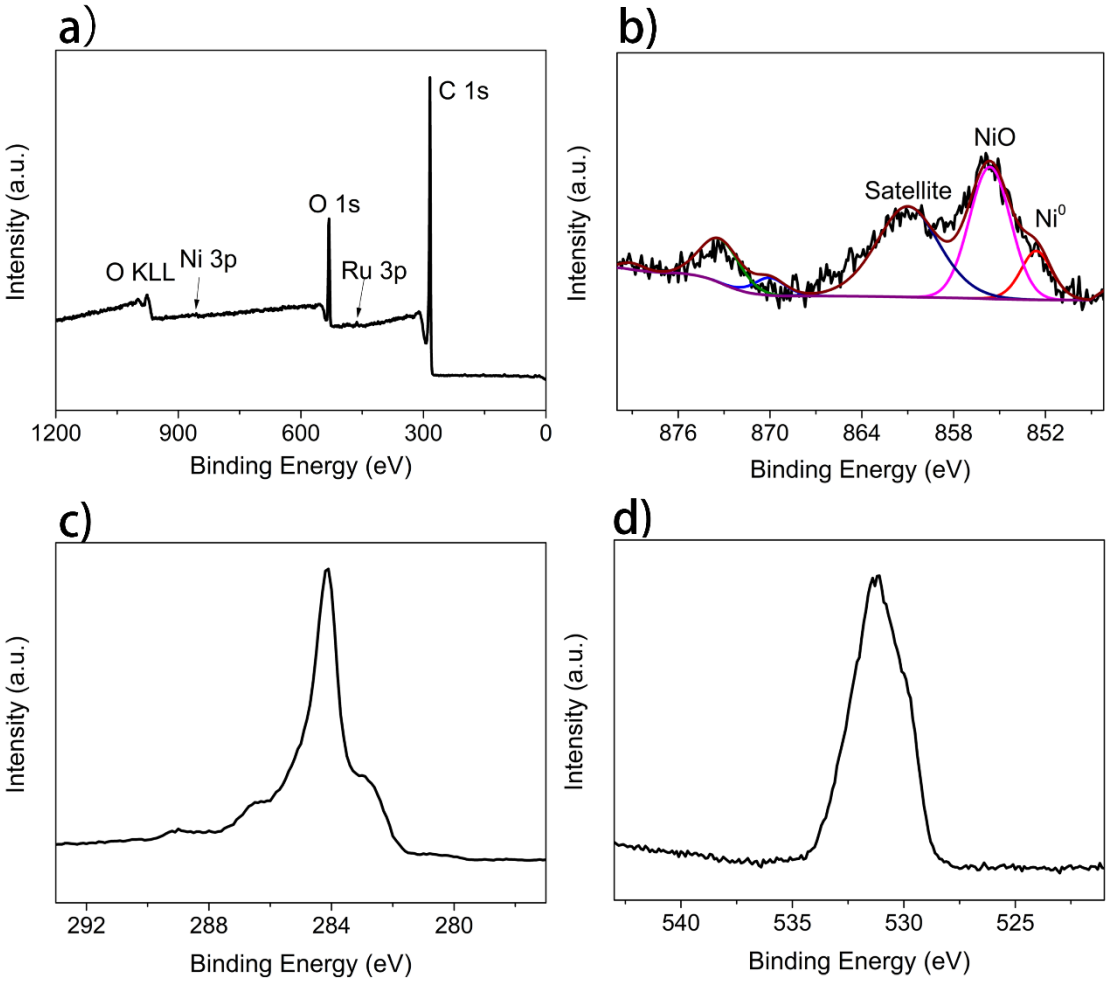

Fig. S5 The XPS spectra of Ni_3-Ru_{10}/C catalyst: a) survey spectrum; b) Ni 2p XPS spectrum; c) C 1s XPS spectrum; d) O 1s XPS spectrum.

Table S3 The influences of alcohol hydrogen donors for CTH of HMPO into δ-Lactams (MPO) over Ni_3-Ru_{10}/C catalyst.[a]

Ent.	Solvent	**MPO** yield (%)[b,c]	**DPA** Yield (%)[b,c]
1	MeOH	-	-
2	EtOH	5.3	-
3	1-PrOH	6.5	-
4	2-PrOH	83.5	14.8
5	2-BuOH	63.7	-
6	cyclohexanol	14.2	-
7	t-BuOH	-	-
8	t- pentanol	-	-

a) Reaction conditions: **HMPO** (125 mg, 1 mmol), Ni_3-Ru_{10}/C catalyst 60 mg, alcohol 2 mL, N_2 1.5 MPa, 180 °C/ 12 h; b) **MPO** and **DPA** yield were determined by GC with decane as the internal standard; c) **HMPO**: 4-hydroxy-6-methylpyridin-2(1H)-one, **MPO**: 6-methylpiperidin-2-one, **DPA**: diisopropylamine.

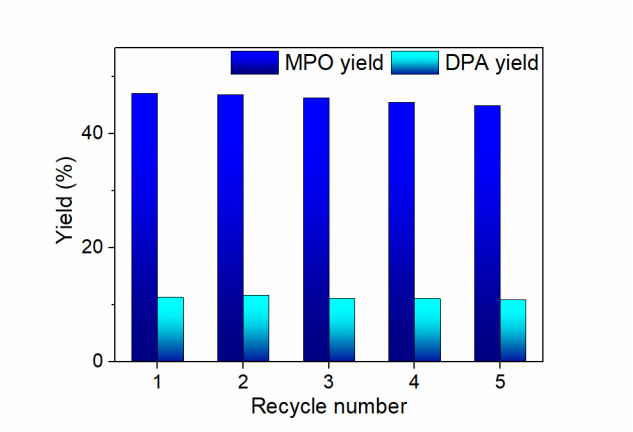

Fig. S6 The recyclability of Ni_3-Ru_{10}/C catalyst at the initial stage, reaction conditions: HMPO 2 mmol, catalyst 120 mg, 2-PrOH 4 mL, N_2 1.5 MPa, 180 °C, 3 h.

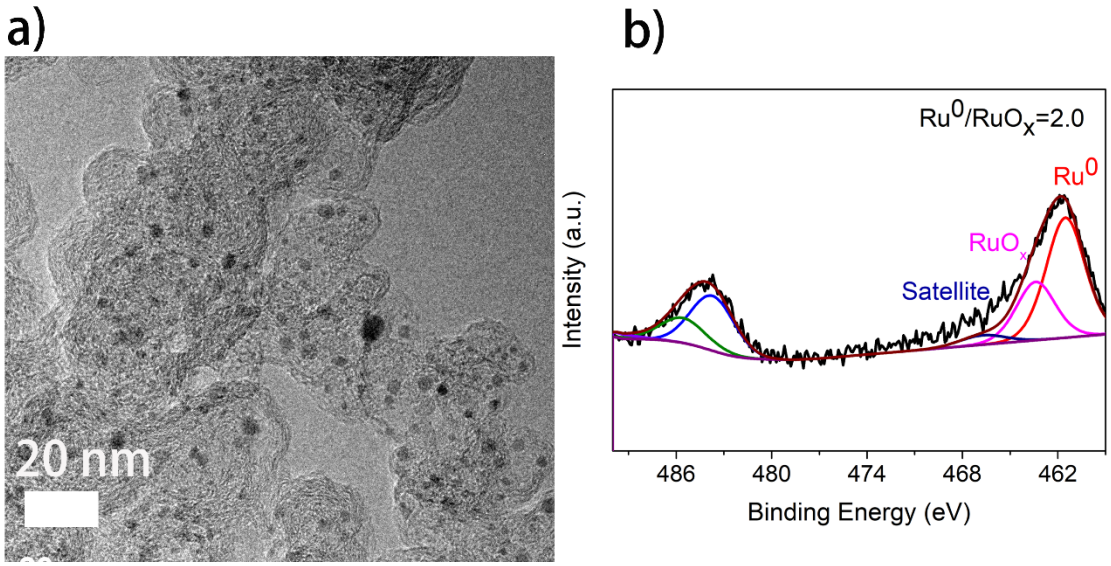

Fig. S7 a) TEM image and b) Ru 3p XPS spectroscopy of the recovered Ni_3-Ru_{10}/C catalyst after reusing for five times.

Fig. S8 GC-HRMS spectra of the reaction mixture for CTH of HMPO using Ni_3-Ru_{10}/C catalyst.

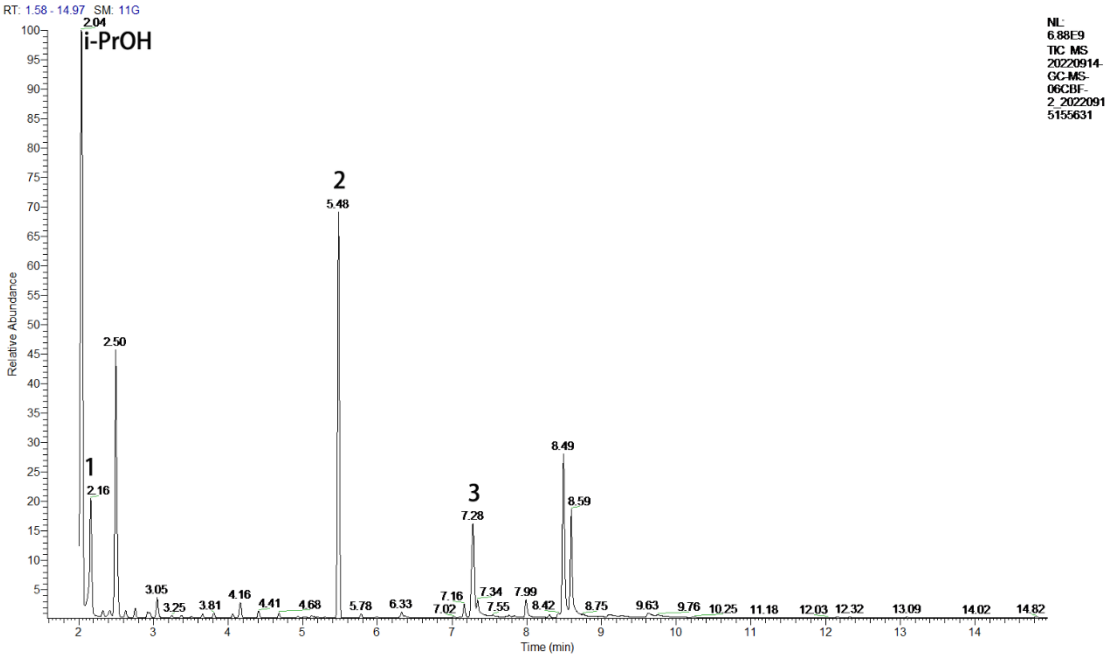

1

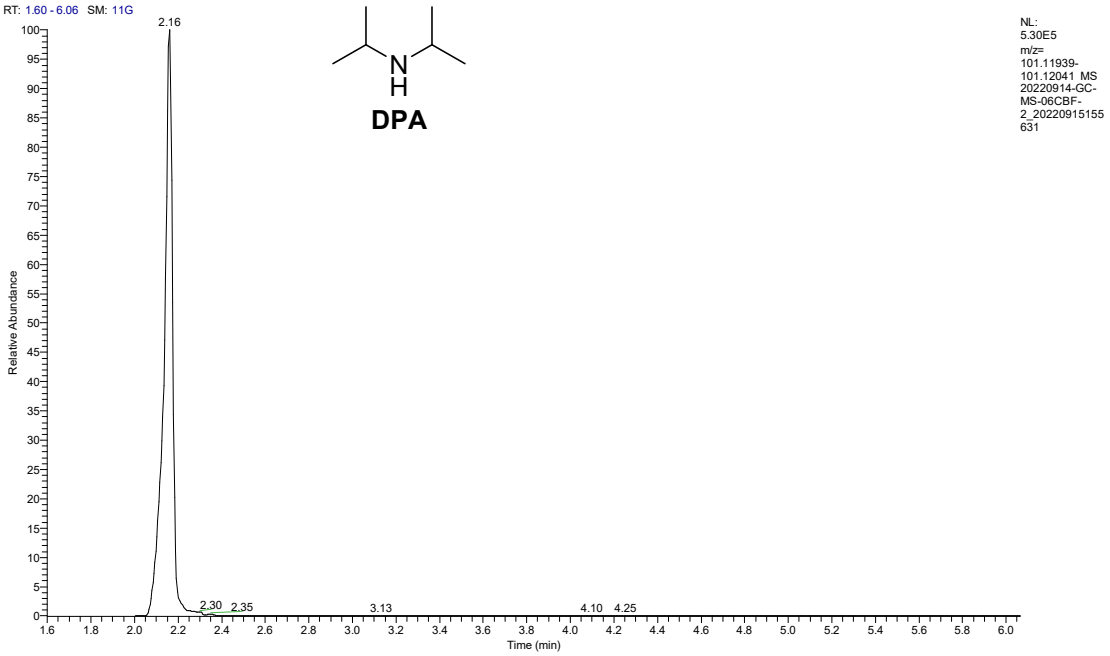

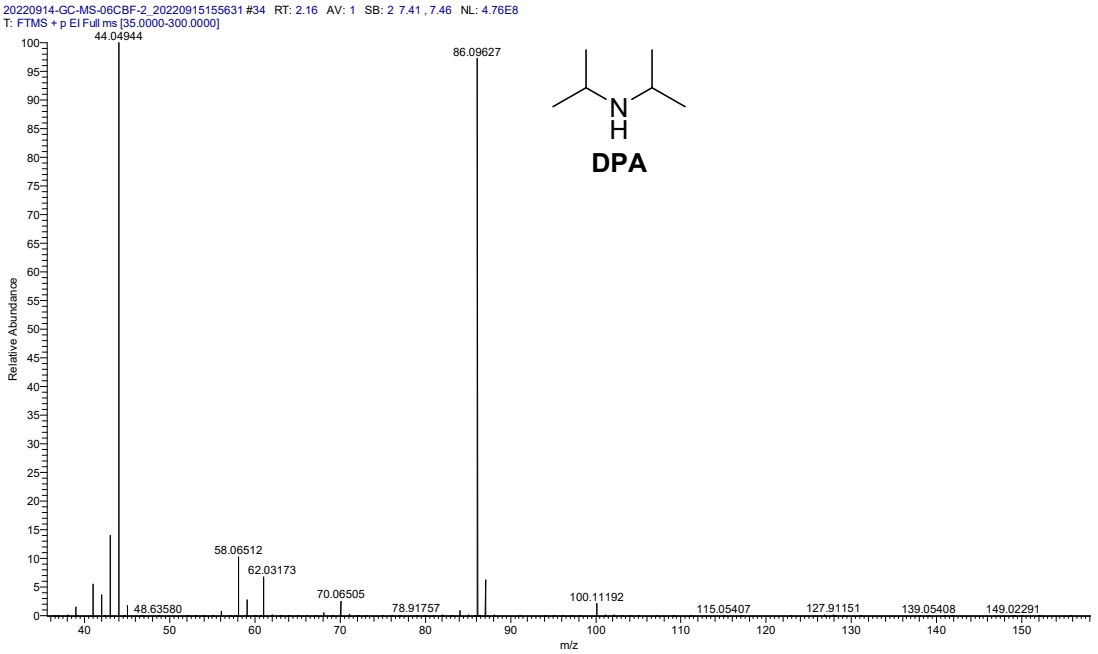
20220914-GC-MS-06CBF-2_20220915155631 #34 RT: 2.16 AV: 1 SB: 2 7.41 , 7.46 NL: 4.76E8
T: FTMS + p EI Full ms [35.0000-300.0000]
44.04944
86.09627
58.06512
62.03173
70.06505
48.63580
78.91757
100.11192
115.05407
127.91151
139.05408
149.02291
Relative Abundance
m/z
DPA

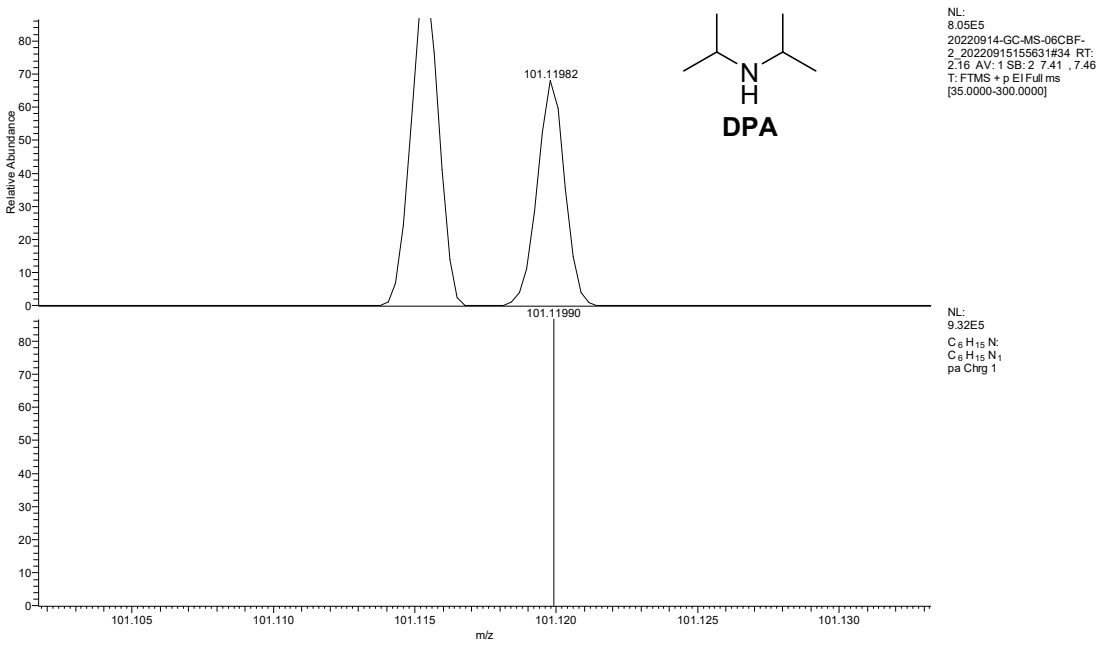
101.11982
101.11990
Relative Abundance
m/z
DPA
NL:
8.05E5
20220914-GC-MS-06CBF-2_20220915155631#34 RT: 2.16 AV: 1 SB: 2 7.41 , 7.46
T: FTMS + p EI Full ms [35.0000-300.0000]
NL:
9.32E5
C6H15N:
C6H15N1
pa Chrg 1

2

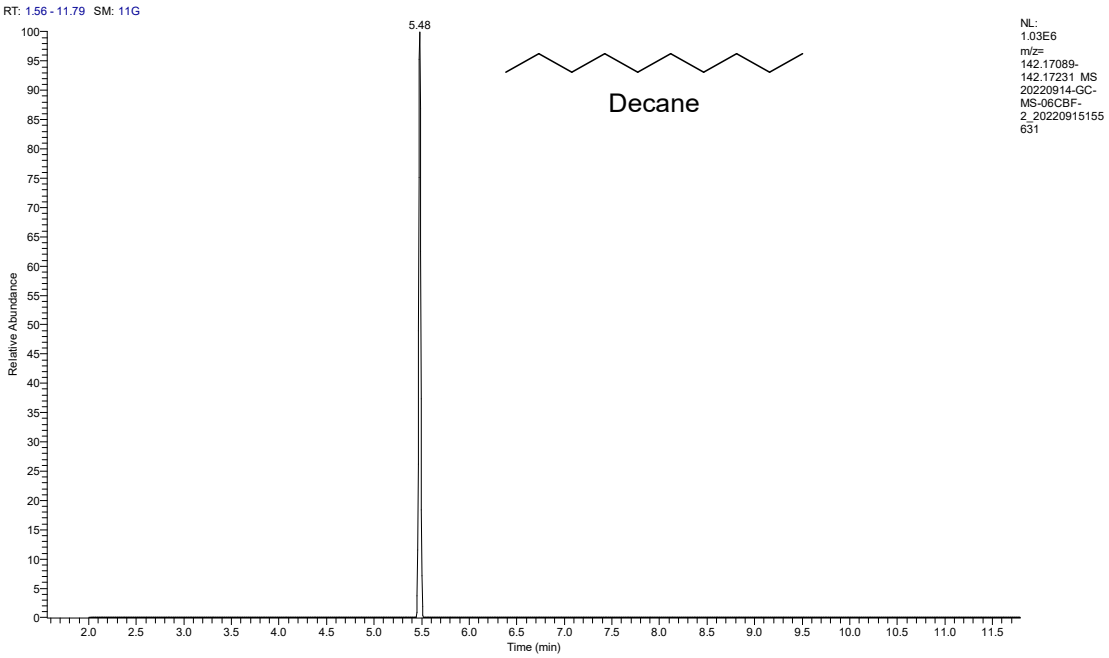
RT: 1.56 - 11.79 SM: 11G
5.48
Decane
NL:
1.03E6
m/z=
142.17089-
142.17231 MS
20220914-GC-
MS-06CBF-
2_20220915155
631
Relative Abundance
Time (min)

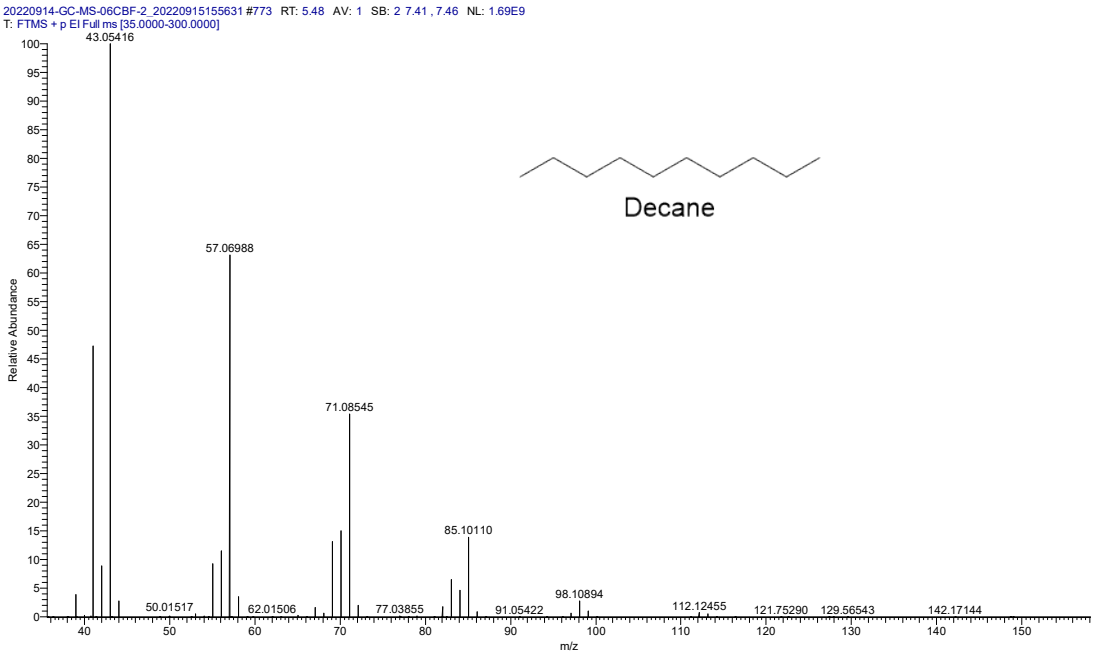
20220914-GC-MS-06CBF-2_20220915155631 #773 RT: 5.48 AV: 1 SB: 2 7.41 , 7.46 NL: 1.69E9
T: FTMS + p EI Full ms [35.0000-300.0000]
43.05416
Decane
57.06988
71.08545
85.10110
98.10894
50.01517
62.01506
77.03855
91.05422
112.12455
121.75290
129.56543
142.17144
Relative Abundance
m/z

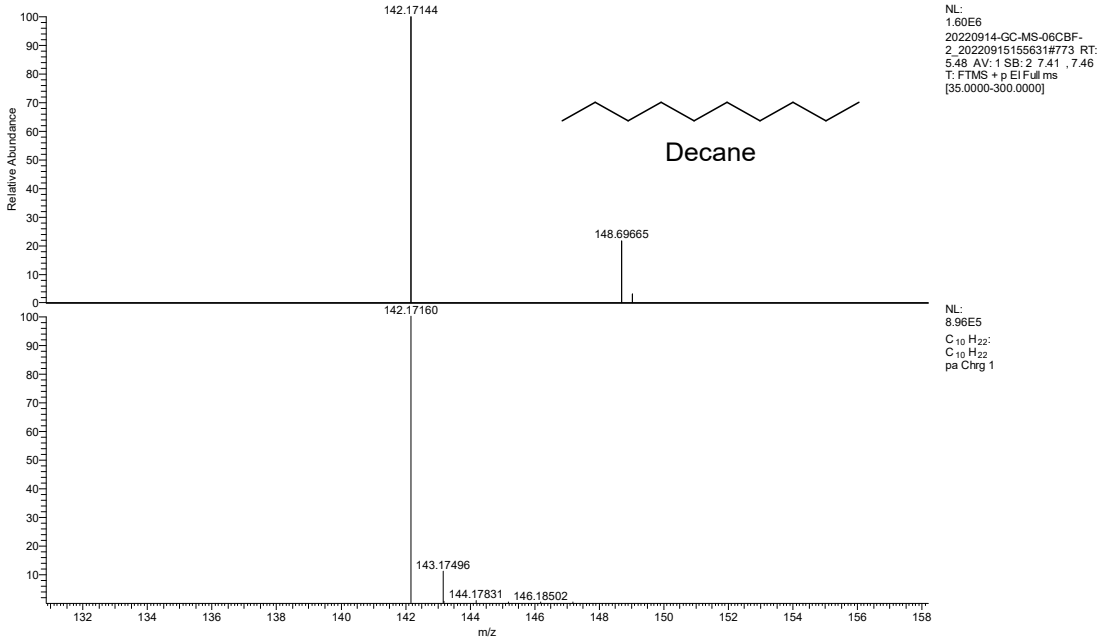
142.17144
148.69665
142.17160
143.17496
144.17831
146.18502
Relative Abundance
m/z
Decane
NL:
1.60E6
20220914-GC-MS-06CBF-2_20220915155631#773 RT: 5.48 AV: 1 SB: 2 7.41 , 7.46 T: FTMS + p EI Full ms [35.0000-300.0000]
NL:
8.96E5
C10 H22:
C10 H22
pa Chrg 1

3

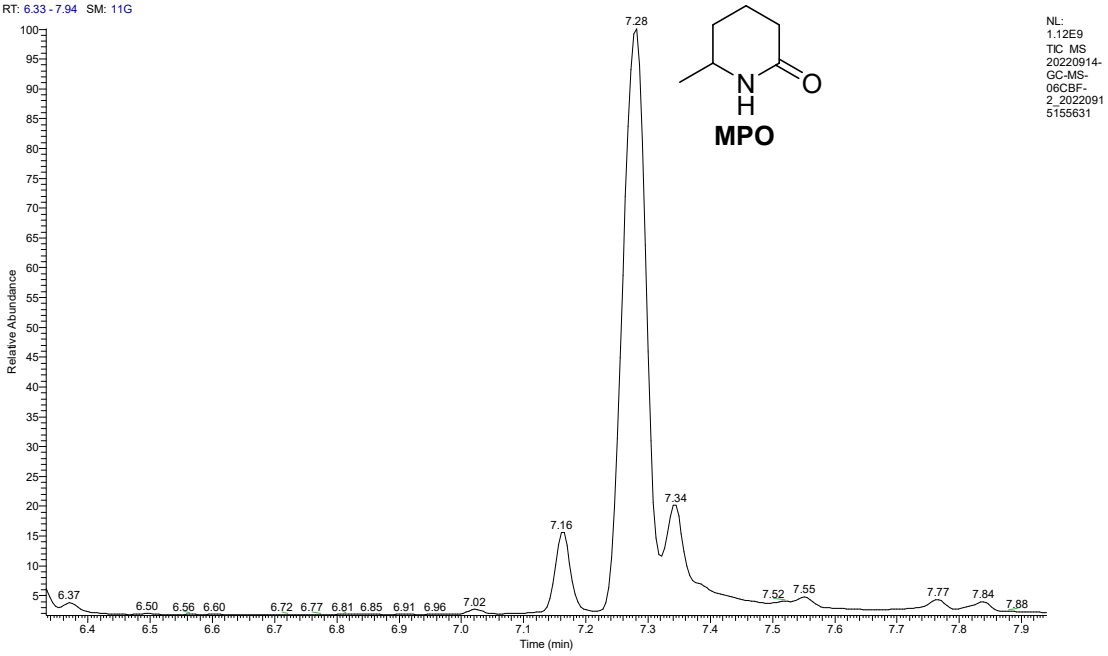
RT: 6.33 - 7.94 SM: 11G
7.28
7.34
7.16
6.37
6.50
6.56
6.60
6.72
6.77
6.81
6.85
6.91
6.96
7.02
7.52
7.55
7.77
7.84
7.88
Relative Abundance
Time (min)
MPO
NL:
1.12E9
TIC MS
20220914-GC-MS-06CBF-2_20220915155631

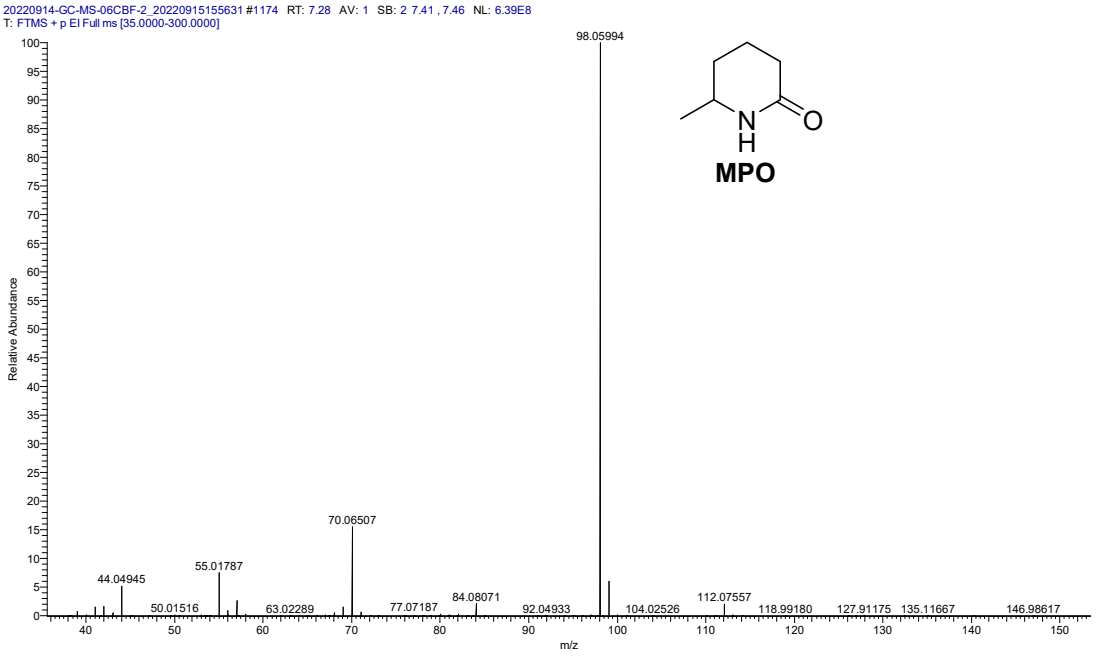
20220914-GC-MS-06CBF-2_20220915155631 #1174 RT: 7.28 AV: 1 SB: 2 7.41 , 7.46 NL: 6.39E8
T: FTMS + p EI Full ms [35.0000-300.0000]
98.05994
70.06507
55.01787
44.04945
50.01516
63.02289
77.07187
84.08071
92.04933
104.02526
112.07557
118.99180
127.91175
135.11667
146.98617
Relative Abundance
m/z
MPO

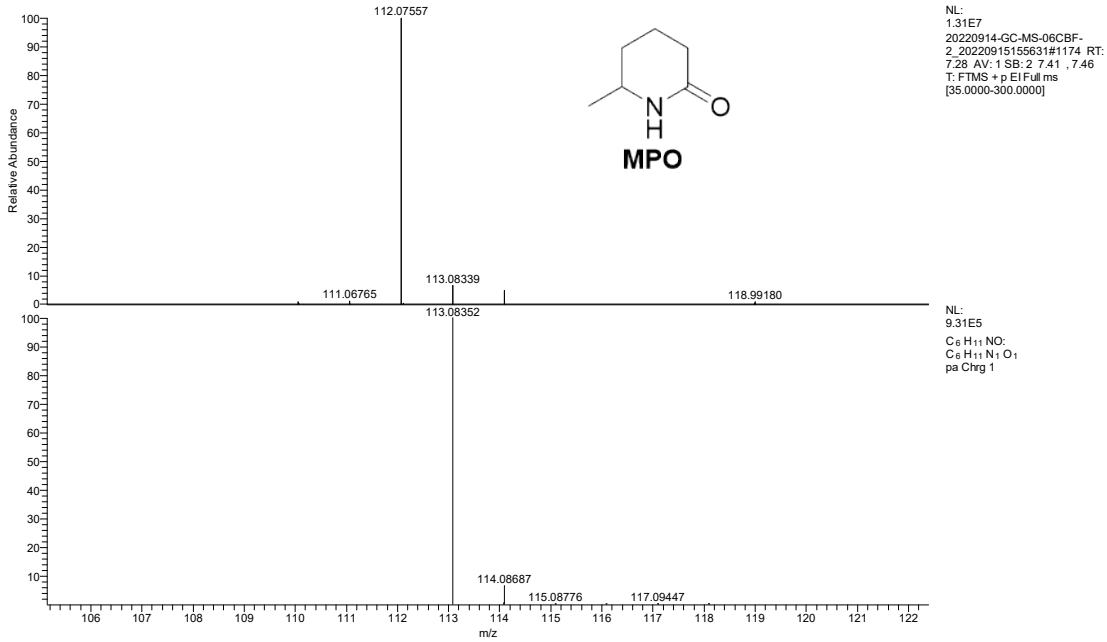
112.07557
111.06765
113.08339
118.99180
113.08352
114.08687
115.08776
117.09447
Relative Abundance
m/z
MPO
NL:
1.31E7
20220914-GC-MS-06CBF-2_20220915155631#1174 RT: 7.28 AV: 1 SB: 2 7.41 , 7.46
T: FTMS + p EI Full ms [35.0000-300.0000]
NL:
9.31E5
C6 H11 NO:
C6 H11 N1 O1
pa Chrg 1

3. Supplementary references

1. B. Chen, Z. Xie, F. Peng, S. Li, J. Yang, T. Wu, H. Fan, Z. Zhang, M. Hou, S. Li, H. Liu and B. Han, *Angew. Chem. Int. Ed.*, 2021, **60**, 14405-14409.